

DESIGN OF COOLING AND VENTILATION FOR TELECOMMUNICATION SHELTER AT HIGH
ALTITUDE

By

PALAK PATEL

Presented to the Faculty of the Graduate School of

The University of Texas at Arlington

in Partial Fulfillment

of the Requirements

for the Degree of

MASTER OF SCIENCE IN MECHANICAL ENGINEERING

THE UNIVERSITY OF TEXAS AT ARLINGTON

MAY 2015

Acknowledgements

I would like to express my deepest appreciation to supervising professor Dr. Dereje Agonafer for motivating and encouraging me. Without his guidance and persistent help this thesis would never have been completed. I would also like to thank him for providing me exposure to international conferences.

I would also like to thank Dr. A. Haji-Sheikh and Dr. Kent Lawrence for serving as my committee members. I thank Ms. Sally Thompson her continuous help in several educational matters. Ms. Sally was very quick at replying emails. I thank Debi Barton for guiding in all advising, enrolling class and for process of thesis defiance.

In addition, I thank Mr. David Bartek and Mr. Chuck Mann from CommScope for sharing their technical knowledge during my study. I am thankful to Betsegaw Gebrehiwot and Manasa Sahini for their invaluable support in completion of this work. I learnt a lot from Betsegaw Gebrehiwot.

Finally, I thank my parents who have encouraged me and sponsored my graduate studies. My special gratitude towards my friends' enthusiasm and support in completion of my study.

April 22, 2015

Abstract

DESIGN OF COOLING AND VENTILATION FOR TELECOMMUNICATION SHELTER AT HIGH ALTITUDE

Palak Patel, MS

The University of Texas at Arlington, 2015

Supervising Professor: Dereje Agonafer

Telecommunication shelters house information technology (IT), networking, power, and cooling equipment such as racks, power cabinets, batteries, fans, etc. For reliable operation of the IT and networking equipment, shelters need to satisfy or exceed minimum environmental guidelines for all equipment they contain. These guidelines typically contain specified operational temperature, maximum gaseous and particular contaminant levels.

In this work, cooling and ventilation needs of a telecommunication shelter at an altitude of 9,678 feet are studied by modeling the system and simulating various operational and weather scenarios using FloVENT 10.1, a computational fluid dynamics (CFD) tool. The shelter contains two compartments: the IT compartment and the battery compartment.

The IT compartment contains Electronic equipment which generate specific amount of heat. The battery compartment contains three Lead Acid Gel Type battery strings. During charging of the batteries, Hydrogen gas is generated which is released into the shelter. Sufficient ventilation is needed to keep the level of Hydrogen in the shelter under 2% concentrations by volume level.

Amount of Hydrogen generation by the batteries and heat dissipation by all electronic components in the shelter varies during day or night time. This study contains the worst case scenarios during winter and summer which are studied assuming steady state conditions. Due to accumulation of hot air and hydrogen near roof line, Exhaust is shifted to top and also two small holes are created to provide proper ventilation. Supplemental heating is provided for winter to keep temperature at desired level. By providing inlet blowers and above briefed ventilation, it has been noticed that maximum temperature and hydrogen level is achieved as desired.

Table of Contents

Acknowledgements	ii
Abstract	iii
List of Illustrations	vi
List of Tables	viii
Chapter 1 Introduction	1
1.1 Telecommunication shelter with photovoltaic	1
1.1.1 Working of System using photovoltaic	2
1.2 Need for CFD code	3
1.3 Motivation for work.....	3
Chapter 2 Computational fluid dynamics analysis	5
2.1 Introduction	5
2.2 Governing Equations	5
2.3 Solution Methodology	6
2.4 Turbulence Modeling	8
2.4.1 LVEL Algebraic Turbulence Model.....	8
2.4.2 Clapped LVEL Turbulence Model	9
2.4.3 LVEL K-Epsilon Turbulence Model	9
2.5 FloVENT smart parts	9
2.5.1 Cuboid & Prism.....	9
2.5.2 Enclosure.....	10
2.5.3 Rack	10
2.5.4 Recirculation.....	10
2.5.5 Source	10
2.5.6 Sloping block	10
2.5.7 Resistance.....	11
2.5.9 Region	11
Chapter 3 Shelter Description.....	12

3.1 Model description.....	12
3.1.1 IT compartment	13
3.1.1.1 Details of electronic equipment	16
3.1.2 Battery compartment	19
3.2 Grid independence study.....	23
Chapter 4 Experimental characteristic of exhaust gravity dampers	24
4.1 Introduction	24
4.2. Experimental set up	24
4.2.1 Introduction to air flow bench	24
4.2.2 Experimental set up guidelines	25
4.3 Angle vs. CFM	26
4.4 CFD modeling.....	29
4.5 System Resistance Curve	29
Chapter 5 Results	33
5.1 Summer model	33
5.1.1 Base model inlet conditions.....	33
5.2 Improved summer model.....	37
5.3 Winter model.....	39
5.3.1 Base model conditions	39
5.4 Winter improved model.....	40
Chapter 6 Conclusion and future work.....	44
6.1 Conclusion and Discussion.....	44
6.2 Future work.....	44
References.....	45
Biographical information	46

List of Illustrations

Figure 1.1 Example of PV telecomm shelter.....	2
Figure 1.2 Working of PV Telecomm shelter	3
Figure 2.1 Discretization	7
Figure 3.1 Top view of model.....	12
Figure 3.2 Isometric view of model	13
Figure 3.3 Fan curve for inlet blowers.....	15
Figure 3.4 Air flow through blower assembly	15
Figure 3.5 Performance curve for MERV filters	16
Figure 3.6 4" MERV 11 filter.....	17
Figure 3.7 P Q curve for power cabinet fans	17
Figure 3.8 Air flow through power cabinet	18
Figure 3.9 Detail of IT compartment	19
Figure 3.10 Battery.....	20
Figure 3.11 Isometric view of modelled battery	21
Figure 3.12 Detail of battery compartment.....	22
Figure 3.13 Exhaust gravity damper assembly.....	22
Figure 3.14 Grid independence study on improved design	23
Figure 4.1 Experiment set up on air flow bench.....	25
Figure 4.2 Exhaust assembly set up on air flow bench	26
Figure 4.3 Angle measurement set up on air flow bench	27
Figure 4.4 Picture taken at time of 2340 CFM	28
Figure 4.5 Volume flow rate Vs Angle of exhaust gravity dampers	28
Figure 4.6 Isometric view of exhaust assembly for system resistance curve	29
Figure 4.7 Comparison of system resistance curve.....	32
Figure 5.1 Temperature plot of summer base model.....	35
Figure 5.2 Concentration plot of summer base model.....	36
Figure 5.3 Particle trace of summer base model	37

Figure 5.4 Placement of monitored volume region	37
Figure 5.5 Temperature plot for summer improved model	38
Figure 5.6 Particle trace of summer improved model	38
Figure 5.7 Concentration results comparison for summer	39
Figure 5.8 Battery temperature of winter base model.....	40
Figure 5.9 Placement of heater.....	41
Figure 5.10 Temperature plot for winter improved model.....	41
Figure 5.11 Particle trace for winter improved model	42
Figure 5.12 Concentration for winter improved model.....	43

List of Tables

Table 3.1 Heat loading of electronic equipment.....	13
Table 4.1 CFM VS Angle from experiment	27
Table 4.2 Comparison of CFD and Experimental results for exhaust assembly	31
Table 5.1 Solver set up	34
Table 5.2 Ambient conditions for air in summer.....	34
Table 5.3 Ambient condition for Hydrogen.....	35
Table 5.4 Monitor point's temperature for summer base mode	36
Table 5.5 Monitor point's temperature for summer improved model	38
Table 5.6 Ambient condition of air for winter.....	39
Table 5.7 Monitor point's temperature for winter improved model.....	42

Chapter 1

Introduction

1.1 Telecommunication shelter with photovoltaic

Telecommunication shelters house information technology (IT), networking, power, and cooling equipment such as racks, power cabinets, batteries, fans, etc. They are located in outdoor environment. The main purpose of it is to protect electronic equipment from humidity, dust, moisture, solar radiation, etc. This is because telecommunication equipment is typically exposed to outdoor environment. The housed electronic equipment generates heat and there is impetus to keep inside air temperature within prescribed limits. It depends on critical factors such as ambient temperature, heat dissipation by housed components, location of inlet and exhaust, etc. Hence, prescribed temperatures are maintained within the enclosures for optimum performance of the electronics equipment.

In remote areas where power grid is not nearby, there is need for PV telecommunication system. It can be used for inaccessible sites where it is extremely expensive or impossible to connect to the grid. Such system has large Photo Voltaic arrays or modules attached to the building which absorb sunlight and convert it during day time into electricity. The valuable feature of PV systems is to have ability to connect to existing power grid. Such telecommunication systems consist of solar energy systems and storage batteries to power the telecom DC loads for 24 hours a day. Storage batteries produce certain amount of hydrogen while it is charging or discharging, the hydrogen production increases significantly which needs to be ventilated.



Figure 1.1 Example of PV telecomm shelter

1.1.1 Working of System using photovoltaic

A solar Photovoltaic array, battery, and charge controller are the three primary components of the PV system. The solar array generates DC power for the load and charges the battery, which serves as the energy storage device that powers the load when there is no output from the array. The charge controller regulates the output of the PV array and ensures proper charging of the battery, thus protecting it from abuse. Output from the solar modules varies considerably, depending on the prevailing sunlight and temperature conditions. Therefore, it's required to regulate its output by wiring it to the charge controller before it goes on to the battery bank and loads. Once the batteries are fully charged, the charge controller doesn't let current from the PV modules flow into them. Similarly, once the batteries have been drained to a certain predetermined level, the charge controller will not allow more current to be drained from the batteries until they have been recharged.

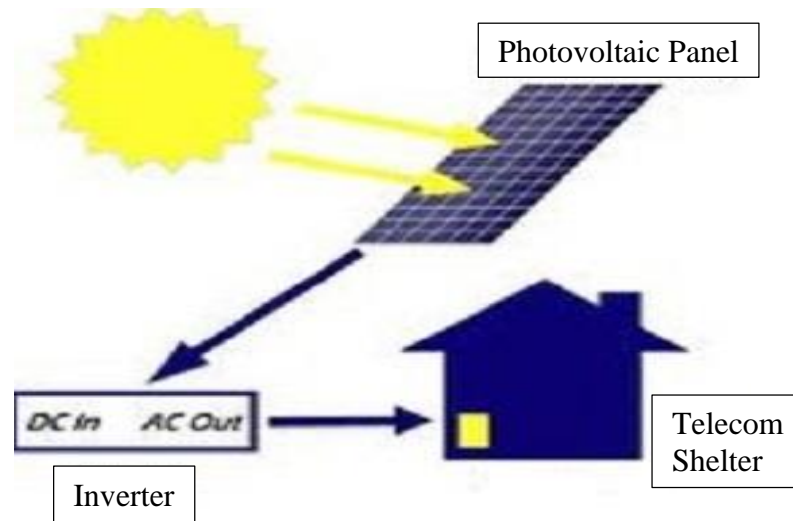


Figure 1.2 Working of PV Telecomm shelter

1.2 Need for CFD code

CFD code gives some predictive computer based outcome to engineer. It helps engineer to analyze results before actually implemented product into market. The necessity of CFD code has been increased drastically for designers. It helps designers in reducing time to market product.

The accuracy of the CFD code depends on a number of factors namely the algorithm used, method of discretization, grid size, time steps involved and the mode of heat transfer. Thus various thermal design options and its impact on the system can be simulated and studied, avoiding the need for experimental work thereby saving time and money.

The objective of CFD is to provide the engineer with a computer-based predictive tool that enables the analysis of the air-flow processes occurring within and around buildings, with the aim of improving and optimizing the design of new or existing heating or ventilation systems.

1.3 Motivation for work

Remote sites are invariably harsh environments with temperature and humidity varying widely throughout the year. Due to changes in climate, it is important to have thermal and air flow management inside shelters. The daily air temperatures exceeding 50°C in middle eastern deserts,

which combined with internal heat generation from the telecom equipment make the inside telecom shelter prone to temperature as high as 80°C. In these conditions, electronic equipment will not function properly. The cooling system design needs to be tailored to the type of environmental conditions the shelter will be placed in as well as the heat generation by the equipment installed inside the shelter. The goal of the designer is to maintain the peak temperatures in the shelter below a certain level, which is normally prescribed by the electronic equipment manufacturer. For this shelter, all of the electronic equipment in the shelter is designed to work between an ambient condition between -20°C and +50°C.

All lead acid batteries, particularly flooded types, will produce hydrogen under both normal and abnormal operating conditions. A primary consideration for any user is considering a flooded battery solution centers on the issue of hydrogen evacuation. In addition to the primary focus on human and system safety, Hydrogen also impacts battery life and maintenance economics, much of which centers on maintaining proper concentrations in the flooded battery. Hydrogen explosion range is 4.1% to 72%. So it is better to have Hydrogen below 4% though designing sufficient ventilation. The manufacturer recommends optimum temperatures to maximize the life of the batteries, and acceptable limits that must be maintained. Ideally, lead acid batteries should be maintained between +15°C and +25°C. Exposure to temperatures outside of this range, and the duration of those exposures will have the effect of reducing the life expectancy of the batteries. The maximum operating range for lead acid batteries is roughly 0°C to +50°C. Any exposure above +30°C will have a significant impact on life expectancy.

Commercial building ventilation systems are typically designed to provide slight pressurization to minimize infiltration. This pressurization is achieved by having the outside or makeup air flow rate higher than the exhaust or relief air flow rate. Moreover, Hot air from electronic equipment and Hydrogen evacuation has to be removed from proper ventilation system. It should be remembered however that hydrogen is lighter than air, and will therefore be an increased risk at higher elevations. All these factors matters while designing ventilation system for such shelter.

Chapter 2

Computational fluid dynamics analysis

2.1 Introduction

Computational Fluid Dynamics (CFD) deals with the numerical simulation of fluid flow, heat transfer and chemical reactions. CFD uses numerical methods and algorithms to solve and analyze problem. A numerical prediction is a consequence of the mathematical model representing the physical domain of interest. Computers are used to compute governing equations with boundary conditions. Equations are solved iteratively as steady state or transient condition. This CFD study involves the system level electronics like the telecommunication shelters, the housed equipment, battery compartment and the surrounding conditions like the ambient temperature and solar heat load.

The objective of CFD is to provide the engineer with a computer-based predictive tool that enables the analysis of the air-flow processes occurring within and around electronics equipment. This technology has widely been applied to various engineering applications such as automobile, aircraft HVAC, and weather science.

2.2 Governing Equations

FloVENT10.1 uses primitive variable treatment in that the field variables it solves are:

- u , v and w , the velocity resolute in Cartesian coordinate directions x , y and z ,
- p the pressure,
- T the temperature of the fluid and/or solid materials.

These variables are functions of x , y , z and time. The differential equations which satisfy these field variables are called conservation equations.

The numerical solution for heat transfer and fluid flow based problems are obtained from solving a series of three differential equations along with necessary equation for this study. These governing differential equations are the conservation of mass, conservation of momentum and conservation of energy, equation of concentration and state equation.

For a generalized case the conservation of mass is given by:

$$\frac{\partial \rho}{\partial t} + \nabla \cdot (\rho \vec{V}) = 0$$

The conservation of momentum for a generalized case is given by:

$$\rho \left[\frac{\partial \vec{V}}{\partial t} + (\vec{V} \cdot \nabla) \vec{V} \right] = -\nabla p + \nabla \cdot \vec{\tau} + \rho \vec{f}$$

The conservation of Energy for a steady low velocity flow is given by:

$$\rho \left[\frac{dh}{dt} + \nabla \cdot (h \vec{V}) \right] = -\frac{Dp}{Dt} + \nabla \cdot (k \nabla T) + \phi$$

The equation of concentration is given by:

$$\text{Percent by mass} = \frac{\text{mass of solute}}{\text{mass of solution}} \times 100$$

The equation of state,

$$pv = nRT$$

2.3 Solution Methodology

The solution domain is the region of space where the governing equations are solved. The solutions of these equations are obtained by setting the boundary condition for the solution domain.

Boundary conditions applied in this study:

$$\vec{V} \cdot \vec{n} = 0 \text{ At surface}$$

Also, as an incompressible and steady flow: density is constant,

$$\frac{d}{dt} = 0$$

The boundary conditions for this study also include ambient temperature and solar radiation. The conditions at the domain wall of the system also needs to be specified whether they are open, closed (wall) or symmetric. The fluid properties namely conductivity, density, viscosity, specific heat and diffusivity need to be specified [24].

The different techniques that can be used to solve the governing equations are:

- Finite Difference Method: The differential terms are discretized for each element.

- Finite Volume Method (FVM): The governing equations are integrated around the mesh elements whose volumes are considered for the solution.
- Finite Element Method (FEM): The variation of variables within elements is approximated by a function, and a residual is minimized.

The CFD tool used for this study is FloVENT 10.1 which is based on the Finite Volume Method (FVM). In FVM the solution domain is discretized into a number of control volumes or grid cells, where the variables to be calculated is located at the centroid of the finite volume.

FVM works by integrating the differential form of the governing equations over each control volume. The Finite Volume Method has an inherent advantage that satisfies the conservation of mass, momentum and energy.

The discretization results in a set of algebraic equations, each of which relates the value of a variable in a cell to its value in the nearest neighbor cell. The layout for the grid and velocities for a grid having a total of 224(= 7×8×4) cells is shown in Figure 1-1.

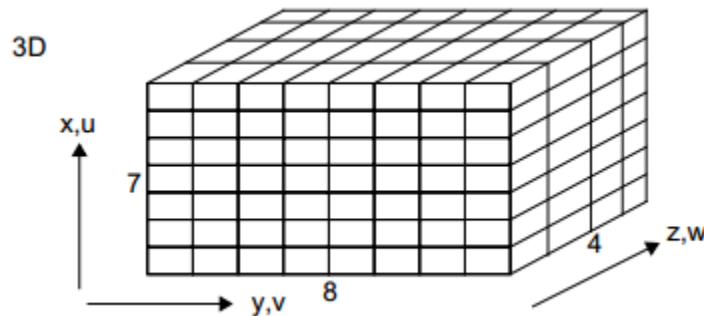


Figure 2.1 Discretization

Taking the example of T, the temperature variable, it is computed by the algebraic equation:

$$r = \frac{C_0 T_0 + C_1 T_1 + C_2 T_2 + C_3 T_3 + C_4 T_4 + C_5 T_5 + C_6 T_6 + S}{C_0 + C_1 + C_2 + C_3 + C_4 + C_5 + C_6}$$

Where

T_0 Temperature value in the old time step

$T_1, T_2, T_3, T_4, T_5, T_6$ Temperature values in the six neighboring cells

C_n denotes the coefficients that link the in-cell value to each of its neighbor-cell values.

If there are n cells in the solution domain, then there are $5n$ algebraic equations to solve as the equation needs to be solved for each field variables T, u, v, w and p .

Normally, fine grid is used in regions of the solution domain where the gradients of the variable are expected to be the high. Finer the grid better the algebraic equations approximates to the governing differential equations. Grid size needs to be small in the area of interest. Many factors affect for getting solution close to real such as grid size, accuracy of boundary conditions, turbulence model.

2.4 Turbulence Modeling

Nature of flow from electronic equipment varies from laminar to turbulent. For representation of turbulence within fluid, it is necessary to estimate turbulent viscosity. It can be evaluated by following formula,

$$\lambda_t = \frac{\mu_t C_p}{Pr_t}$$

In FloVENT, turbulence models can be represented by three different models named LVEL Algebraic Turbulence Model, Clapped LVEL Turbulence Model and LVEL K-Epsilon Turbulence Model.

2.4.1 LVEL Algebraic Turbulence Model

The LVEL algebraic turbulence model removes the need for any user-defined velocity or length scale. The model depends on the calculation of the distance to the nearest wall (L), the local velocity (VEL) and the laminar viscosity to determine the effective viscosity. A velocity scale is taken to be the cell velocity.

A length scale is calculated from the following equation:

$$D = \sqrt{(|\nabla\phi|^2 + 2\phi)}$$

Where $\nabla\phi = -1$ with $\phi = 0$ at a wall.

2.4.2 Capped LVEL Turbulence Model

The Capped LVEL turbulence model is the same as the LVEL Algebraic turbulence model but capped to:

multiplier × laminar viscosity

2.4.3 LVEL K-Epsilon Turbulence Model

The K-Epsilon model is a two equation model that is extensively used for turbulent fluid dynamics. It has been tailored specifically for planar shear layers and recirculating flows. This turbulence model calculates two variables; the kinetic energy of turbulence (k) and the dissipation rate of k (denoted ε).

The eddy viscosity is defined from dimensional analysis as:

$$\mu_T = C_\mu \rho \frac{k^2}{\varepsilon}$$

This model consist two transport equations: first equation is for kinetic energy turbulence (k) and second equation is for dissipation rate of k (ε).

Transport equations are:

$$\frac{\partial(\rho k)}{\partial t} + \frac{\partial(\rho k u_i)}{\partial x_i} = \frac{\partial}{\partial x_i} \left[\left(\mu + \frac{\mu_t}{\sigma_k} \right) \frac{\partial k}{\partial x_i} \right] + G_k + G_b - \rho \varepsilon$$
$$\frac{\partial(\rho \varepsilon)}{\partial t} + \frac{\partial(\rho \varepsilon u_i)}{\partial x_i} = \frac{\partial}{\partial x_i} \left[\left(\mu + \frac{\mu_t}{\sigma_\varepsilon} \right) \frac{\partial \varepsilon}{\partial x_i} \right] + C_{1\varepsilon} \frac{\varepsilon}{k} (G_k + C_{3\varepsilon} G_b) - C_{2\varepsilon} \rho \frac{\varepsilon^2}{k}$$

2.5 FloVENT smart parts

This part of chapter deals with smart parts used for modeling of shelter into FloVENT.

2.5.1 Cuboid & Prism

Cuboid and prism represent solid block. Material, surface, thermal, surface exchange, radiation and grid constraint attributes can be defined to it. Grid is not propagated inside cuboid.

2.5.2 Enclosure

Enclosure shows hollow cuboid surrounded by six walls in which other component can be placed. These walls could be thin or thick and also it can have different materials. Enclosures are created as children of assemblies. In this study, enclosure is used as an outer cover for electronic equipment. There is grid propagation inside enclosure.

2.5.3 Rack

The Rack smart part can represent any row-based or room-based Data Center rack. The main component when modeling a Rack smart part, in addition to the positions of the air supplies and extracts, is the control of the airflow on the faces of the rack. Power dissipation rate and flow type (temperature difference, volume flow rate, non-linear fan) can be attached to Rack smart part.

2.5.4 Recirculation

The recirculation device is a convenient way to represent systems such as fan coil units that recirculate air by extracting it from the enclosure, then conditioning and returning it. The recirculation device is defined by specifying the type and thermal properties of the flow through it, and the location of the air supply (ies) and extract(s). Inlet blowers are represented by recirculation smart part in the study.

2.5.5 Source

Source smart part is used for generating specific amount of pressure, velocity, temperature, concentration or turbulence. It is used for heat generation of electronic equipment and hydrogen generation at the batteries.

2.5.6 Sloping block

Sloping block is used to represent cuboid whose surfaces are not aligned with coordinate axes. With solar radiation on, it is important to attach material surface property to it. Shelter and battery compartment roofs are created with sloping block smart part.

2.5.7 Resistance

Resistance is used for setting the resistance to the air flow distributed across a finite volume or plane. It is used as filter in this study. It is usually placed at inlet to the outdoor enclosure and to particulate contaminants from inlet air. It is also used to restrict amount of solar load falling onto shelter.

2.5.9 Region

Regions are defined spaces in the model. Regions are extensively used to capture summary values such as flow rate, pressure, temperature, heat flux for 2D (collapsed region) or 3D (non-collapsed region) in the visual editor. After solution, the mean flow results as well as the mean, minimum and maximum values for any variable can then be tabulated over this new region using the Visual Editor in Tables mode. Regions are also beneficial to localize grid in the area which do not contain any geometry. One can attach grid constraints to the region.

Chapter 3

Shelter Description

3.1 Model description

Photo Voltaic (PV) telecommunication shelter is situated at 9,678 feet from sea level. PV telecommunication shelter has large photo voltaic array placed outside to store solar load. This solar load is converted into electrical energy. Using solar load for power supply is useful in the area where local power grid is far from site location. The batteries store the energy coming from photovoltaic (PV) arrays and provide 100 percent of the shelter's electricity power needs. Lead acid based batteries are used usually for the purpose of storing energy. The shelter contains two compartments: IT compartment and battery compartment.

The IT compartment is 9 feet higher than battery compartment. The whole construction is made of steel wall on concrete floor pad. Ceiling is shaped as gable roof. The insulation in the structure is 4 inch thick R13 rated in the walls, and R20 values in the ceiling. R value is used to define insulation. For insulation material, the thicker it is, the greater the R value. Conductivity K value may be found from following formula:

$$R \text{ value} = \frac{\text{Thickness}}{K\text{-value}}$$

The whole structure is shown in figure below with air direction.

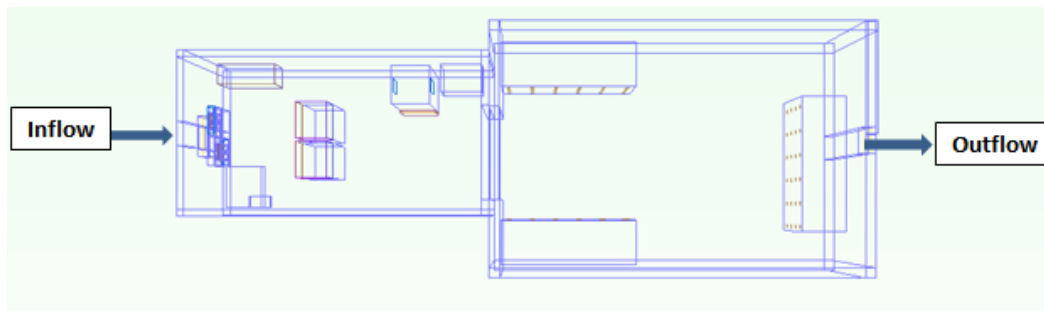


Figure 3.1 Top view of model

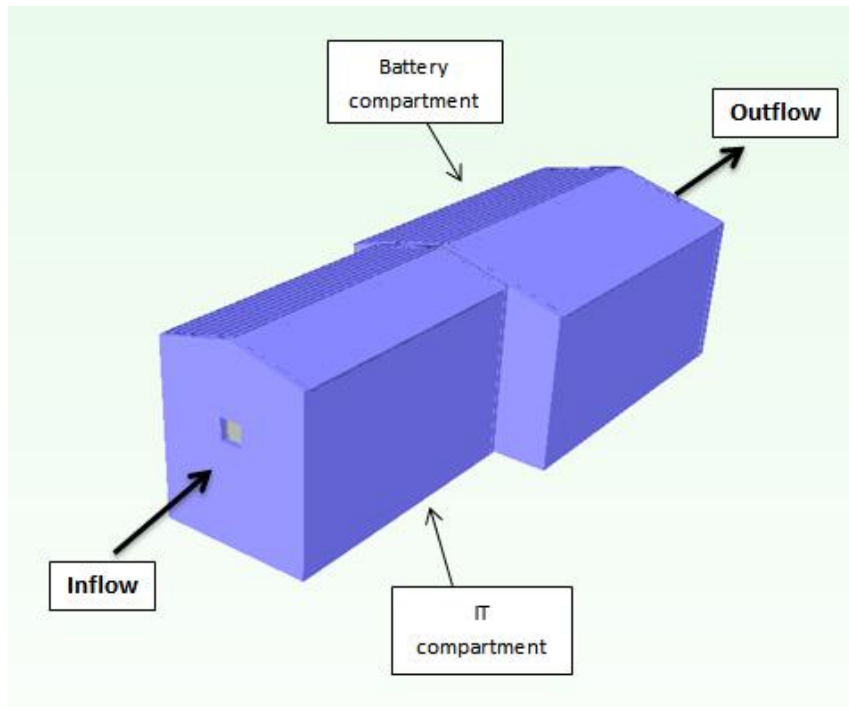


Figure 3.2 Isometric view of model

3.1.1 IT compartment

IT compartment is $9' \pm 2''$ high, $15' \pm 8''$ long and $8' \pm 3''$ wide. The walls and roof of this compartment are 4 inches thick. It has inlet of 30 in^2 area. Main components of the IT compartment include two server racks with one-third of racks populated with servers, a Power cabinet, Inlet blower assembly, a Master DC bus bar, a Starter battery, and an Ericsson radio unit. All electronic equipment in this compartment dissipate specific amount of thermal load. Heat load contributed by each component is given in table below:

Table 3.1 Heat loading of electronic equipment

Unit Name	Heat loading (W)
AT & T racks	3700
Ericsson radio	200
Inlet fan	190
Power cabinet	1350

All IT equipment contribute total of around 5450 W thermal load into shelter. It is important to have cooling and heating load for designing of cooling system. Heating and cooling loads are rates of energy input (heating) or removal (cooling) required to maintain system parameter at desired. Total cooling load is calculated by following formula:

$$Q_{\text{balance}} = Q_{\text{equipment}} + Q_{\text{solar load}} + Q_{\text{cooling}}$$

Solar heat is found from solar intensity given by:

$$Q_{\text{Solar load}} = \text{Projected area} * \text{Solar intensity}$$

Equipment heat load is provided by manufacturer which turns

$$Q_{\text{cooling}} \sim 8054 \text{ W}$$

Depending on requirement of cooling load and volume flow rate, Ebm-papst model R1G280-275542 blower is chosen for cooling this system.

Inlet centrifugal blowers are employed for cooling purpose. Blower assembly contains two impeller blowers which are placed in single tray but at opposite corners. These blowers are Ebm-papst model R1G280-275542 blowers which dissipates 95W of heat each. These centrifugal fans have backward curved blades offering an extremely good aerodynamic efficiency. It extracts air from front side and supplies half through sides. An arrangement for supplying air into shelter has been made to get uniform flow in shelter. Operating point of blowers can be varied depending on system resistance. It is used for air exchange for the shelter. Fan curve is shown below.

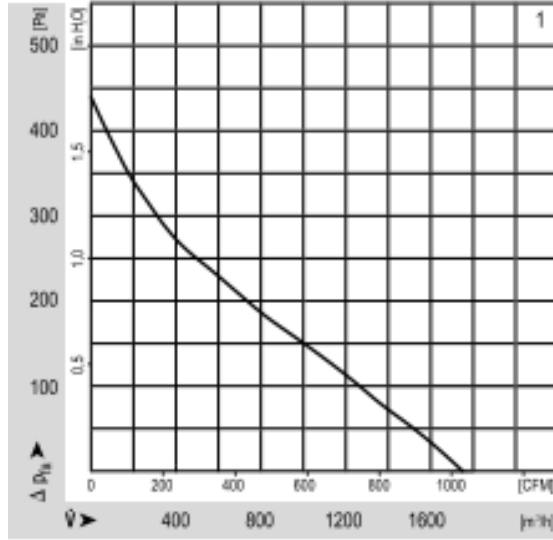


Figure 3.3 Fan curve for inlet blowers

Air flow through blowers is shown in figure below:

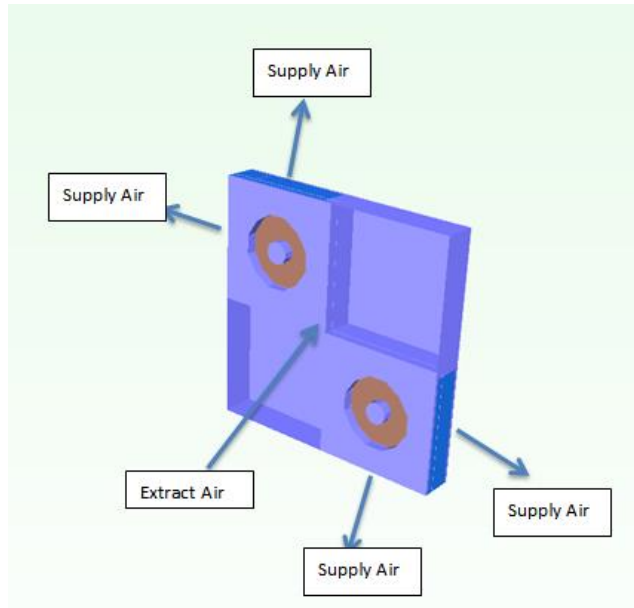


Figure 3.4 Air flow through blower assembly.

3.1.1.1 Details of electronic equipment

Two AT&T racks placed at center, dissipates total of 3500 W of thermal load into shelter. Racks are placed at the height of almost 1.23 m (49 in) from the floor. Each rack is capable of delivering 225 CFM volume flow rate with maintaining 15° C across the rack.

4" Airguard Legacy™ Model LG4-604 MERV 11 Filter is placed at the inlet blower assembly [13]. It has very low resistance which reduces energy consumption. Also, it has high dust holding capacity. Air enters from inlet goes to filter and then blowers. UTA has already tested this filters and results are shown in figure below. Initial resistance of filter is kept as 0.5 from figure below.

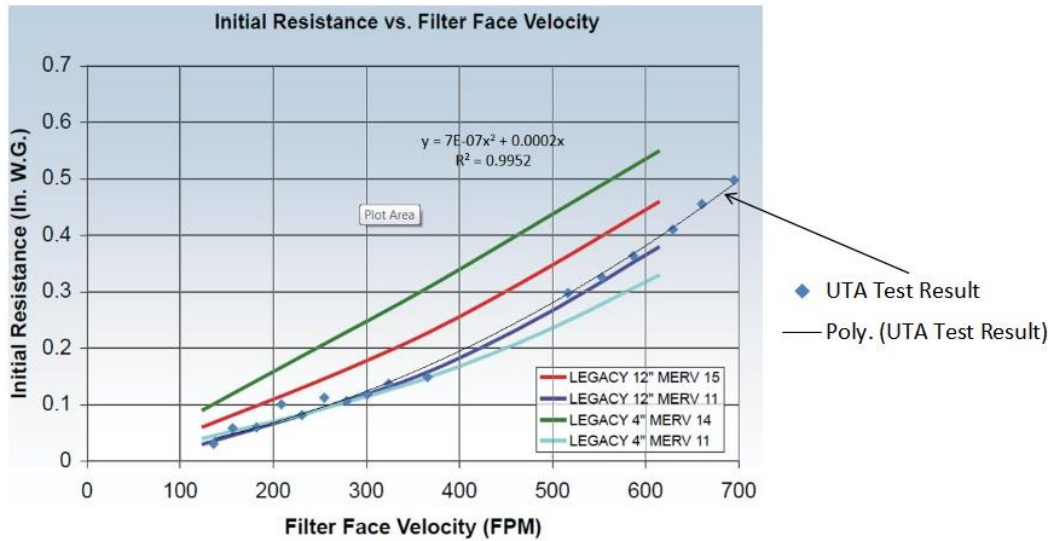


Figure 3.5 Performance curve for MERV filters



Figure 3.6 4" MERV 11 filter

Power cabinet has four fans placed in parallel on same tray. It extracts air from front and exhausts it straight out half- half to both the sides. They are placed 8 inches from the top surface and has a cross-sectional area of 24x8 in². Fan curve is obtained from manufacturer. It is modelled by using advanced planar resistance method described in section 3.1.2 for exhaust assembly.

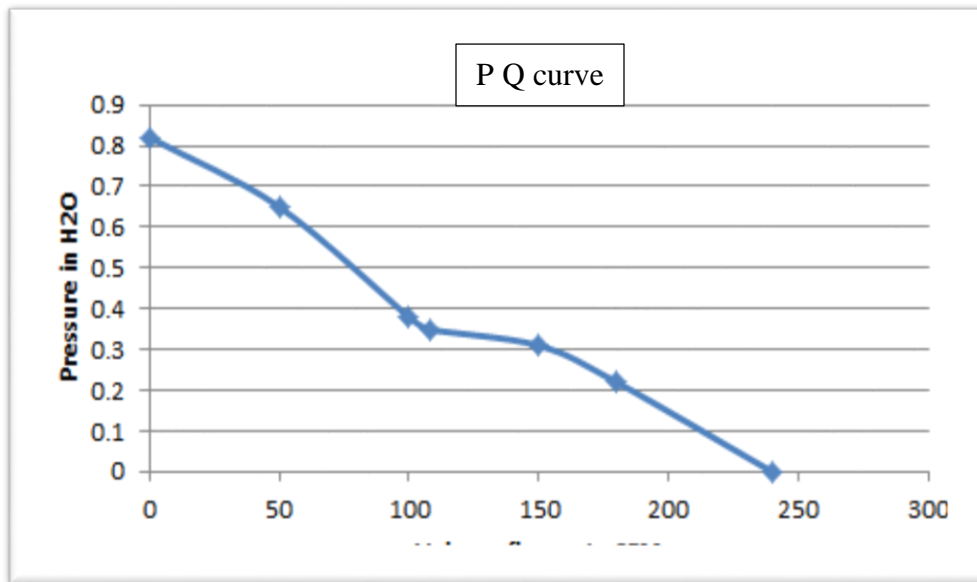


Figure 3.7 P Q curve for power cabinet fans

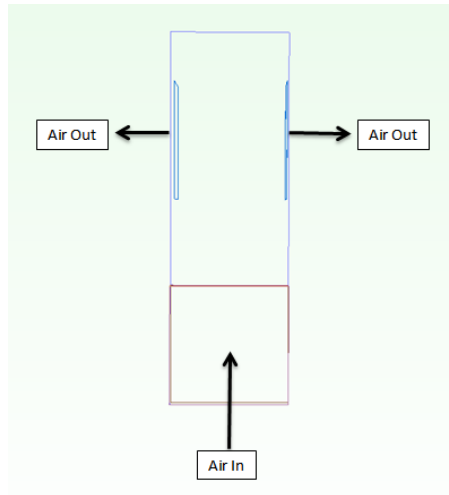


Figure 3.8 Air flow through power cabinet

Also, The Ericsson radio on the side wall consumes 3000W of power, and dissipates 200W of thermal load into shelter. All other components like starter battery, master DC bus bar are passive in contributing thermal load to the shelter. Detail of electronic equipment in IT compartment is shown below.

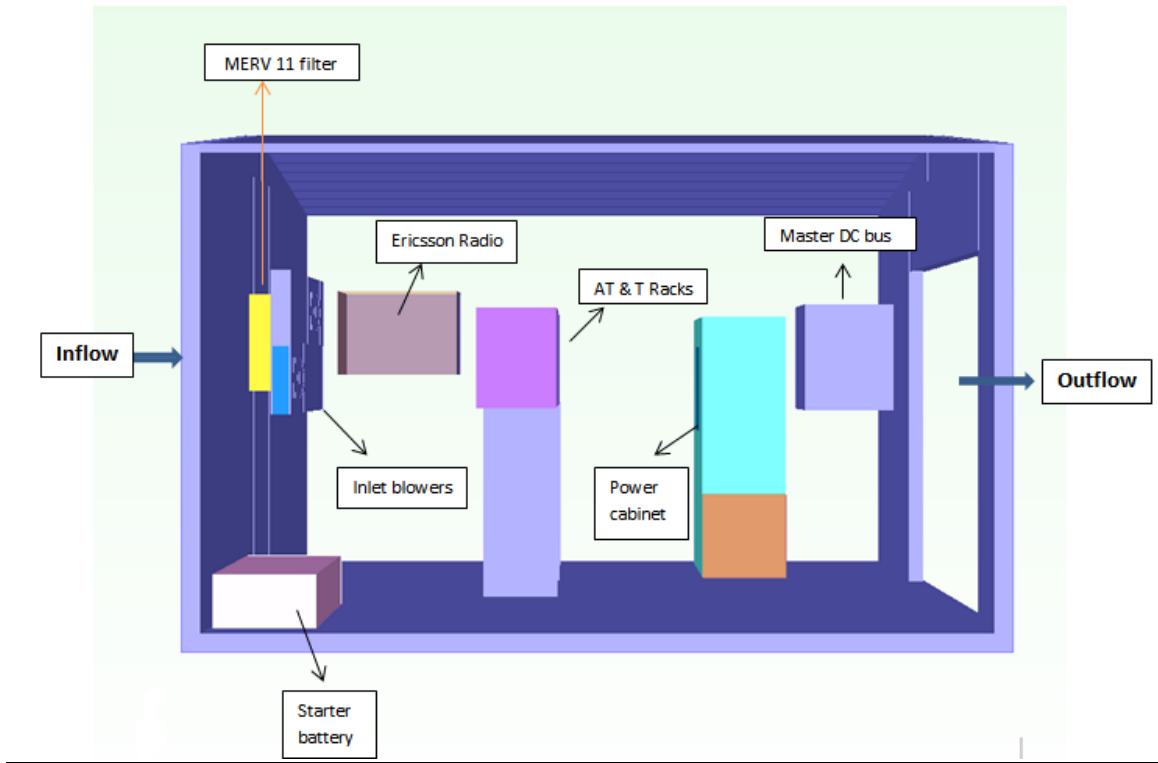


Figure 3.9 Detail of IT compartment

3.1.2 Battery compartment

The battery compartment is attached to IT compartment through passage in between which visible in figure 3.9. It is $8' \pm 5''$ high, $18' \pm 10''$ long and $12' \pm 6''$ wide. The walls of this compartment are 6 inch thick and roof is 2 inch thick. Battery compartment has three 2000AH battery strings and exhaust with louvers. There is passage in between both compartments for communication. Batteries are lead acid gel based which contains 5 ½ % polypropylene (PP), 60% lead (Pb), 25% lead oxide (PbO₂), Silicon Oxide gel.



Figure 3.10 Battery

Each battery string is 1.52 m (60 in) high, 1.12 m (44 in) wide, and 2.95 m (116 in) long, and weighs about 3810 kg (8400 lbs.). Battery produces 200mL/hr./string Hydrogen when it is on float charge or on discharge. When the batteries are being re-charged, especially near full capacity, the hydrogen production increases significantly to 4800mL/hr/string. Detail picture of battery is shown below.

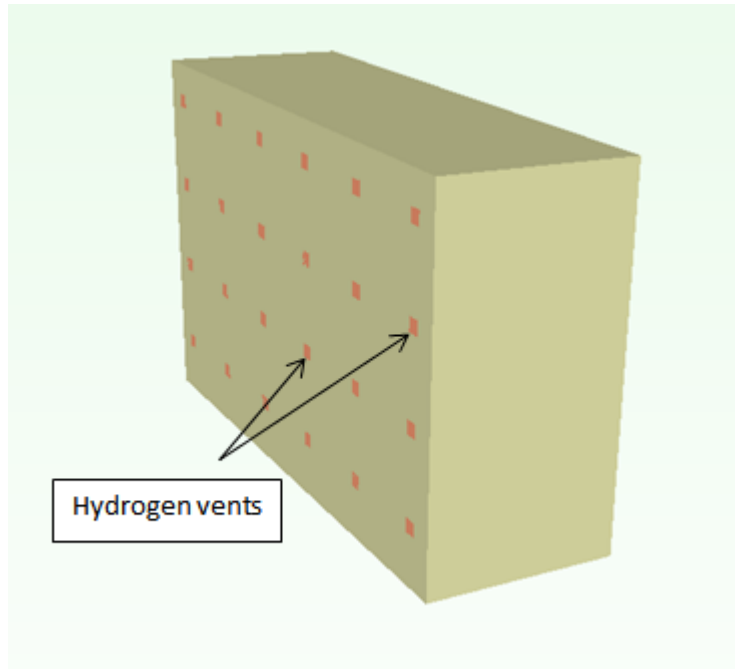


Figure 3.11 Isometric view of modelled battery

Red spots in above picture shows vents which produce Hydrogen. There are three batteries in the battery compartment whose arrangement is shown in figure below. Air will come through door from IT compartment and exist through exhaust provided on the right side of the model. Below is battery compartment figure with monitor point placed on each battery string.

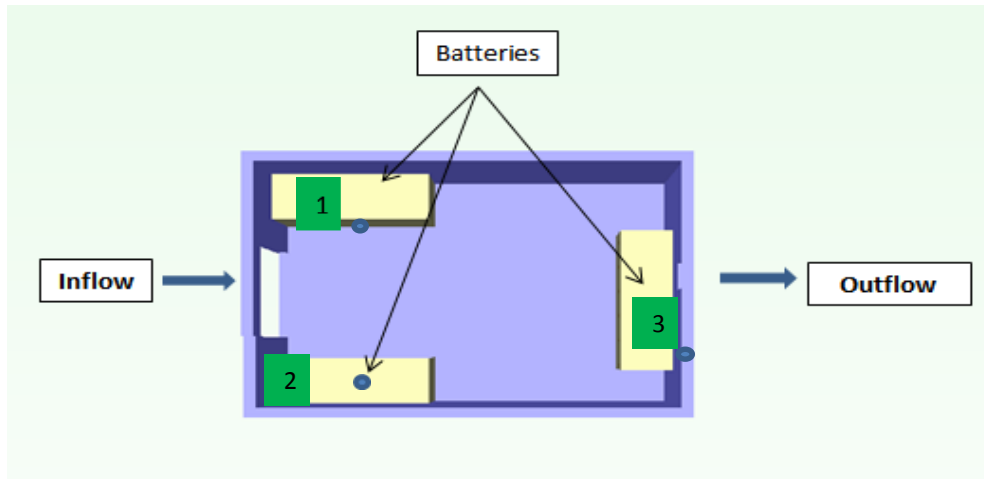


Figure 3.12 Detail of battery compartment

Gravity damper is chosen for the purpose of ventilation at exhaust. Exhaust has 30 in² area. Gravity dampers have shown in figure below. Gravity dampers allow passage for the air from inside of the unit to go towards outside, to prevent overpressure inside unit. It is made up of aluminum. Open area of dampers depends on CFM provided from the inlet unit. If there is no flow then dampers are completely closed. It also prevents dust coming into unit.



Figure 3.13 Exhaust gravity damper assembly

Exhaust assembly is designed using planar resistance in FloVENT. It is used when pressure drop is proportional to exponent of velocity. This allows for the correct modeling of resistances in all flow regimes.

3.2 Grid independence study

Mesh sensitivity analysis has been performed on improved design to ensure the independence of grid. Figure 3.12 shows grid independence in terms of battery string's temperature. It is became independent at 18 million cells but air leakage is found at low cells so all simulations have been done at more than 23 million cells.

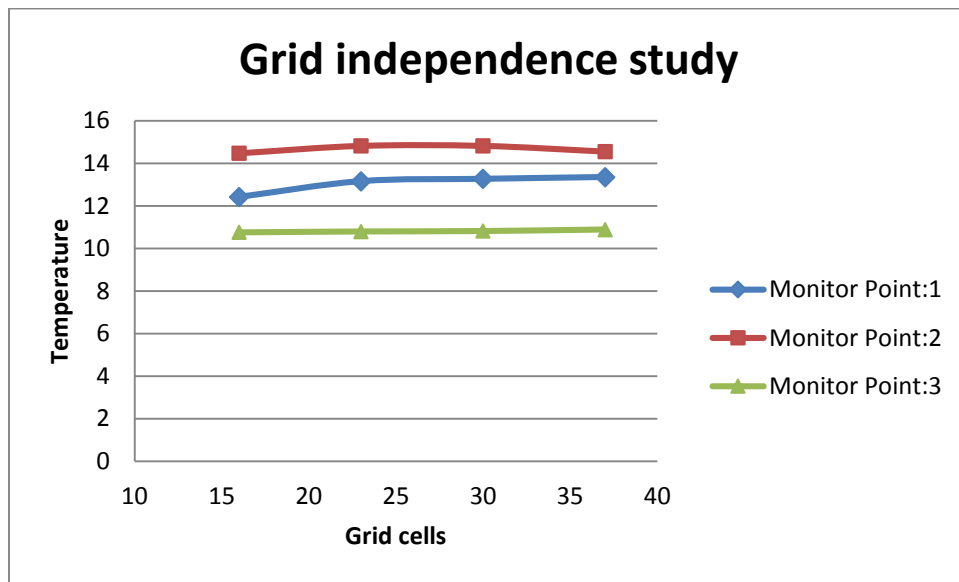


Figure 3.14 Grid independence study on improved design

Chapter 4

Experimental characteristic of exhaust gravity dampers

4.1 Introduction

General ventilation provides and/or exhausts air to provide heat relief, dilute contaminants to an acceptable level, and replace exhaust air. Ventilation could be natural or forced. Industrial areas must comply with ANSI/ASHRAE Standard 62.1-2004 and other standards as required. For this particular application, Gravity ventilation has been implemented. It is highly effective, have low operating costs, do not generate noise, and are self-regulating (i.e. higher heat release increases air flow through ventilators). Care must be taken to ensure positive pressure at ventilators, particularly in heat season. Otherwise, outside air will enter the ventilators.

Having heat sources and radiation heat load inside, adjustable ventilation air gravity damper is used at exhaust to ventilate desired amount of air and hydrogen generated from battery. It is necessary to test exhaust louvers to verify positive pressure at the assembly. This test is performed in air flow bench.

4.2. Experimental set up

4.2.1 Introduction to air flow bench

Air flow bench is used for measuring thermal resistance of a test sample, to calculate air flow rate and for measuring fan performance curve. Air flow bench is generally designed in accordance with AMCA 210-99/ASHRAE 51-1999. The chamber is designed with multiple nozzles to cover full air flow range of the design. The chamber is constructed with pressure taps on each side of the nozzle to measure the differential pressure. These taps are used to measure pressure drops across the system under test. The counter blower is wired to the speed controller from which speed of blower needs to be controlled.

Nozzle array is in the center of the chamber and is accessed through the cover plate. Nozzles are positioned on the plate so that they may be used in parallel to achieve higher flow ranges. Stoppers are provided to block off nozzles not in use and are easily removed for different flow range of testing. The flow range to be covered could be controlled by nozzle.

The chamber has flow straightening screens installed upstream and downstream of the nozzle array. The screens break up turbulence in the air stream and provide a uniform flow approaching the nozzle array.

The flow through the chamber is controlled with a sliding gate valve called a blast gate. By opening the blast gate, the flow is varied through the chamber to provide test data from shut off (no flow) to free delivery (no back pressure) for fan performance evaluation.

4.2.2 Experimental set up guidelines

The exhaust louver which needs to be tested is mounted on the disc at the front of chamber. It should be sealed adequately to prevent leakage. Nozzle is selected based on volume flow rate required for the study. Blast gate kept fully open. Differential pressure and static pressure lines are connected to the multiplexer which is kept inside DAQ.

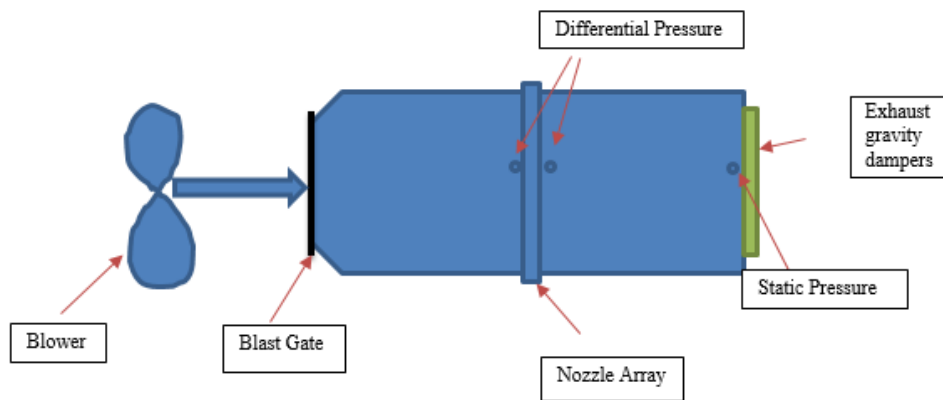


Figure 4.1 Experiment set up on air flow bench

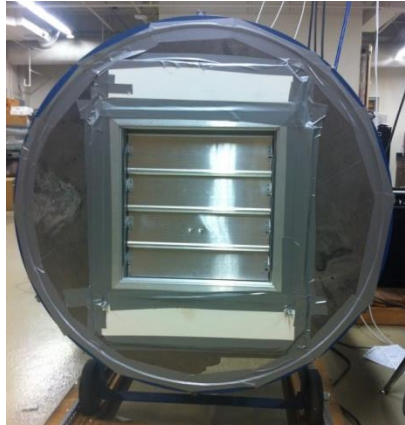


Figure 4.2 Exhaust assembly set up on air flow bench

First data point was at no flow condition which was set as calibration for entire experiment. Also, room pressure and temperature is measured at the time of experiment which was found to be 29.30 in Hg and 24°C +/- 1°C respectively. Start the blower and keep desired speed. Software program collects data from sensor which needs to be used for curve.

4.3 Angle vs. CFM

Angle of louvers depends on Volume flow rate provided. Angle vs. CFM curve helps in understanding of maximum and minimum volume flow rate can be used for the object. This curve is found from experiment setup which includes protractor attached to louvers as shown in figure below.

The following chart shows maximum CFM exhaust assembly handles is 2450 at which louvers open 85°. It is noticed from plot that there is negligible of opening difference of louvers at low range CFM. Full speed of inlet blowers can make louvers to be open at its full.

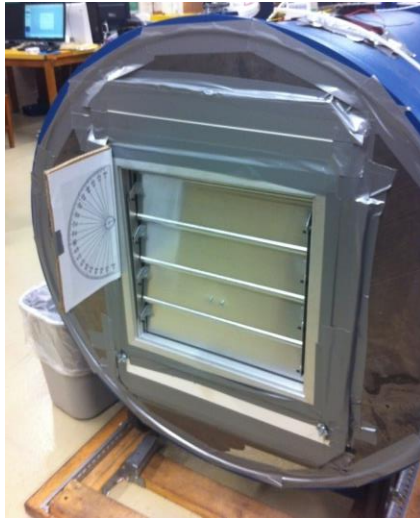


Figure 4.3 Angle measurement set up on air flow bench

Table 4.1 CFM VS Angle from experiment

Flow rate (CFM)	Angle (Degree)
2450	85
2340	79
1857	70
1627	59
1383	54
1234	47
754	35
590	27
430	22
333	15
248	13
120	10

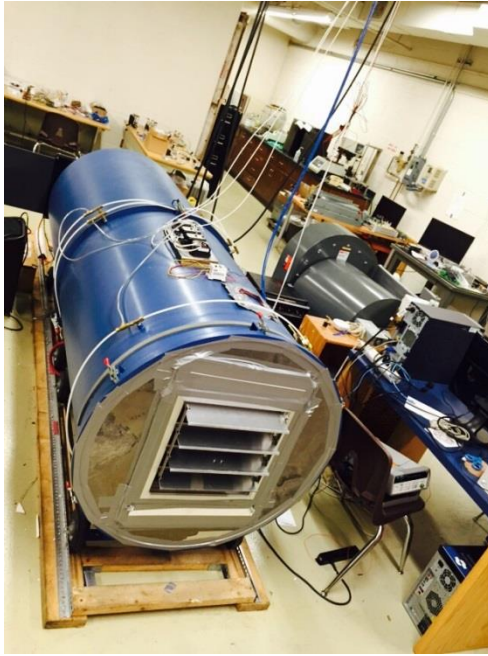


Figure 4.4 Picture taken at time of 2340 CFM

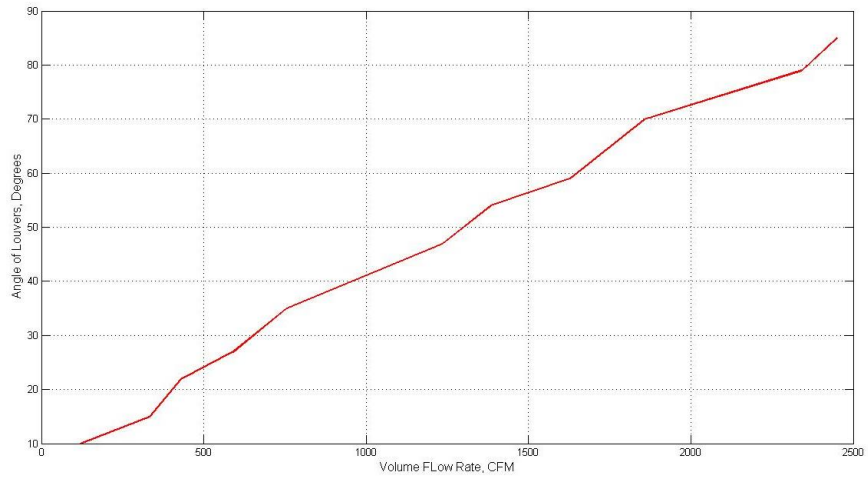


Figure 4.5 Volume flow rate Vs Angle of exhaust gravity dampers

4.4 CFD modeling

Advanced resistance model has been used in place of exhaust louvers to have same behavior in FloVENT 10.1. For the model, A and B coefficients were found using data points collected from experiment. Resistance model is placed at the end of square chamber and rectangular fan is placed at the front side of it. Volume regions were placed upstream and downstream of resistance model to store pressure. The CFD model is shown below in figure.

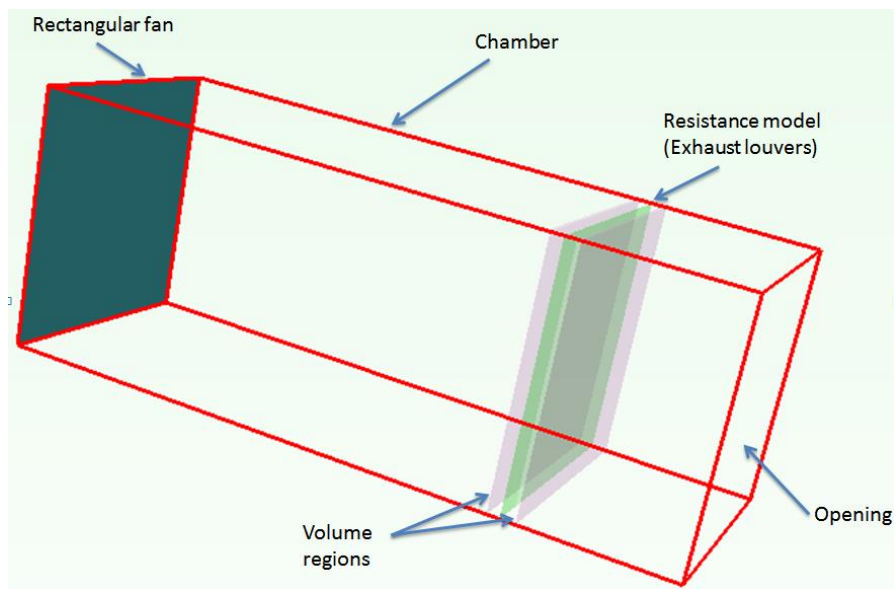


Figure 4.6 Isometric view of exhaust assembly for system resistance curve

Entire simulation is performed using command center. Command center is used to generate and solve different scenarios for the currently loaded project, enabling quickly see the effects of changing project variables. Variation in static pressure in volume region is studied for given volume flow rate (CFM).

4.5 System Resistance Curve

The speed of the blower and the corresponding nozzle diameters are chosen accordingly to achieve flow rates in the range of 120 to 2340 CFM. Both pressure values were sensed and fed to computer program in the experiment. Static pressure sensor values are converted into in Hg by

the information provided on sensor. Differential pressure sensor values are converted into volume flow rate (CFM) from the following formula.

$$Q = 60 \times A \times V$$

Where,

$$Q = \text{Air Flow Rate (m}^3\text{/min)}$$

$$A = \text{Nozzle Sectional Area (m}^2\text{)}$$

$$V = \text{Average Flow Velocity through nozzle (m}^2\text{/sec)}$$

$$V = \frac{2 \times g \times P_n^{1/2}}{r}$$

Where,

$$g = \text{Gravitational acceleration } 9.8 \text{ m/s}^2$$

$$P_n = \text{Differential Pressure}$$

$$r = \text{Specific Gravity of Air (1.2 kg/M}^3 \text{ at } 20^\circ\text{C, 1atm)}$$

Table below shows percentage error between experimental and numerical data. System resistance curve obtained from experiment and CFD is shown in figure below. It can be observed that the flow model is validated with error less than 8%.

Table 4.2 Comparison of CFD and Experimental results for exhaust assembly

Flow rate (CFM)	Static Pressure (in H ₂ O)		Error
	CFD	Experimental	
2340	0.4036	0.4098	1.5%
1857	0.2760	0.2700	2.2%
1627	0.223	0.2125	5.1%
1383	0.1734	0.1636	5.9%
1234	0.1355	0.1305	3.8%
754	0.0711	0.0746	4.6%
590	0.0508	0.0580	-6.6%
430	0.0458	0.0490	-6.5%
333	0.0315	0.0334	-5.6%
248	0.0220	0.0238	-7.5%
120	0.0148	0.0158	-6.3%

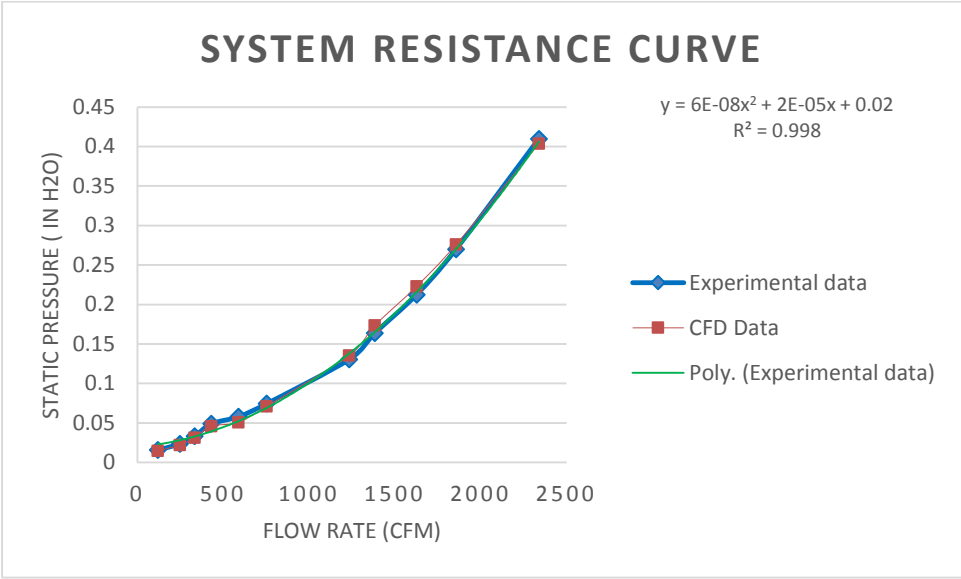


Figure 4.7 Comparison of system resistance curve

Chapter 5

Results

5.1 Summer model

5.1.1 Base model inlet conditions

Solution domain has all wall open boundary condition. Exhaust is created by 45° angle louvers which does not contribute same characteristic as gravity dampers.

Model has been set up for flow and heat transfer. Considering worst case for summer, solar radiation has been turned on. Ambient condition has taken from nearest airport weather data [7]. Humidity is completely ignored at this study. Solar time and date has been specified as 28 July at 5:00 PM with solar intensity of 720 W/m². Azimuth angle and solar altitude is calculated by software itself depending on above data provided. The sun rays are partially reflected and partially absorbed. The amount of heat absorptance is depends on shelter surface. There are two ways to modify solar radiation by cloudiness or by collapsed resistance model. In this model, Solar radiation affects through outer collapsed resistance model of 0.1 free area ratios which means 90% of total solar radiation reflects back.

Plate conduction and double precision solver is turned on in solver set up. For all variables termination residual is set manually. Fan relaxation is set to 0.7 which helps in convergence. The criterion for convergence is to set residuals below 50 and also monitor point's temperature fluctuation within 2° C.

Table 5.1 Solver set up

Variable	Termination residual
Concentration	10^{-5}
Pressure	0.1
X velocity	0.1
Y velocity	0.1
Z velocity	0.1
Temperature	Automatic
KE Turb	Automatic
Diss Turb	Automatic

Ambient conditions are taken from nearest airport weather system to the unit site. Ambient temperature is set to 37° C, pressure is set to 20.83 in Hg and concentration is set to 0. For worst scenario, Hydrogen generation rate is taken as 4800 mL/Hr./string which is provided at battery vents. Density is not kept constant. Ideal gas law is selected so that density is become function of temperature.

Table 5.2 Ambient conditions for air in summer

Ambient air temperature	37° C
Ambient pressure	20.83 in Hg
Conductivity	0.0269 W/m K
Viscosity	$1.88e-05$ Ns/m ²
Density type	Ideal law
Molecular weight	28.966
Specific Heat	1007 J/Kg K

Hydrogen properties is shown in table below. Density of hydrogen is also kept as function of temperature.

Table 5.3 Ambient condition for Hydrogen

Conductivity	0.187 W/m K
Viscosity	9.09e-06 M s/m ²
Density type	Ideal gas law
Molecular weight	2
Specific Heat	14310 J/kg K

5.1.2 Base model results

Minimum size of mesh is kept 0.4 in for this model. Total number of grid cells are 27 million and maximum aspect ratio is 9.99. Ideally, it is better to have aspect ratio less than 10. Mean temperature in shelter is found 49.95° C. Battery strings temperature is found to be 46°-47°C. Operating point for inlet blowers are found as 715 CFM each. Temperature plot is shown below with solar radiation direction.

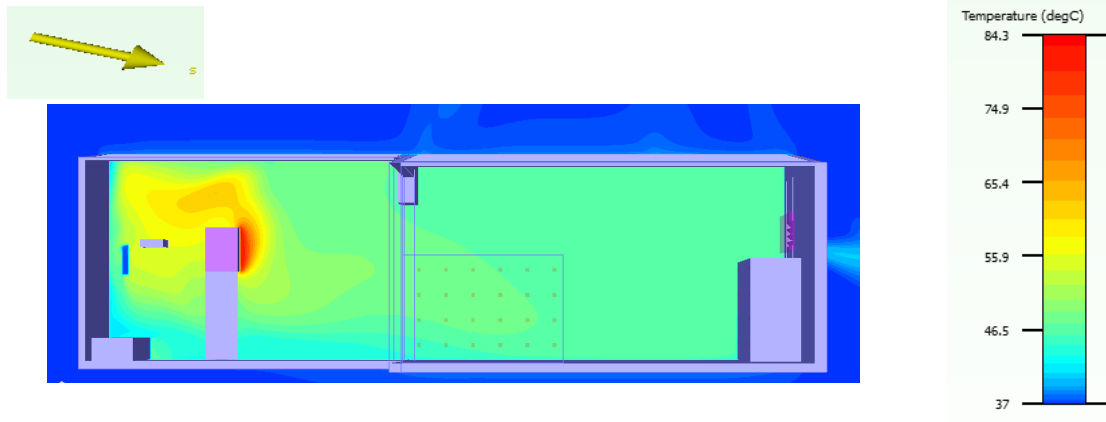


Figure 5.1 Temperature plot of summer base model

Table 5.4 Monitor point's temperature for summer base mode

Monitor Point:1	46.88° C
Monitor Point:2	46.78° C
Monitor Point:3	46.31° C

Concentration plot shows maximum of 2.19% mass which is converted to 30.66% volume at sources which is ignored. As hydrogen is lighter than air, it accumulates near roof line. 17.6% by volume is found near roof. Also, battery temperature is found to be 46-47° C which is in desired range.

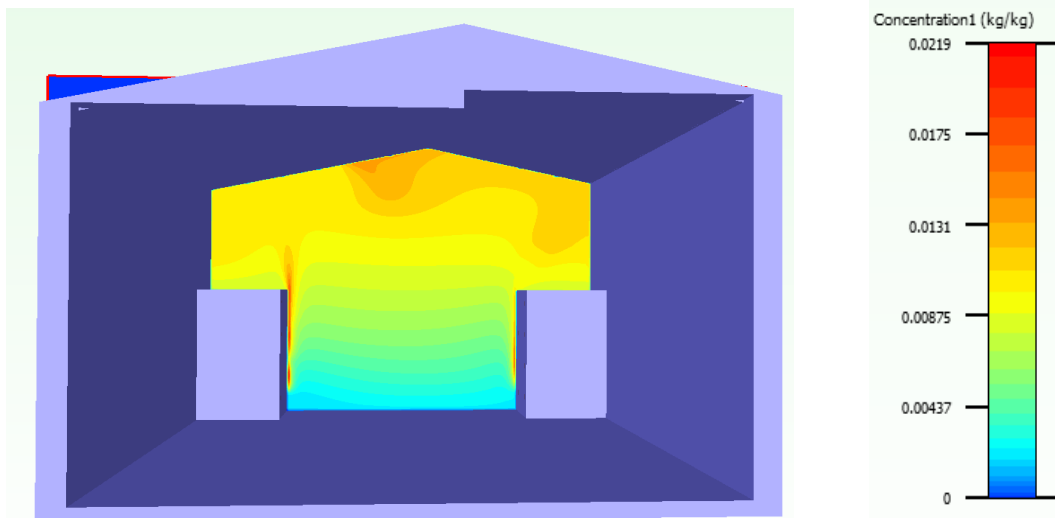


Figure 5.2 Concentration plot of summer base model

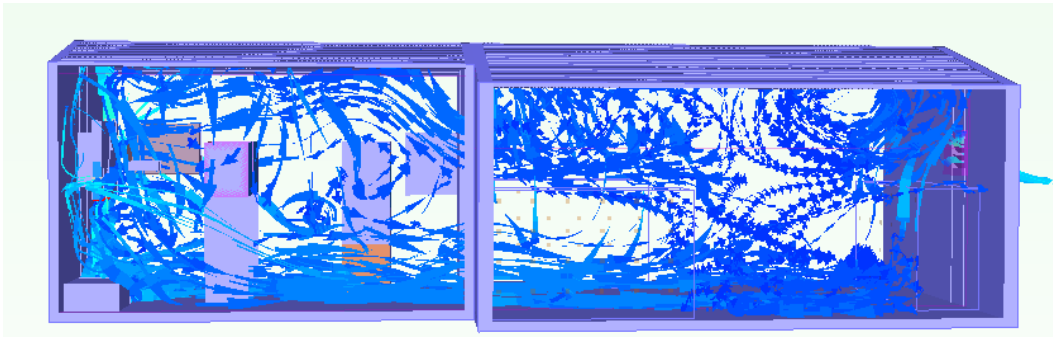


Figure 5.3 Particle trace of summer base model

5.2 Improved summer model

From the results of base model, it is seen that hot air and hydrogen is accumulating near roof. Exhaust is relocated to top and middle of the model to take heat out of the shelter. Density of hydrogen is less than hot air so hydrogen is accumulating near roof which leads to create holes on roof. Location of holes is chosen depending on vents position. They are created exact on the top of vents to exhaust most of the hydrogen. In reality, there will be one way valve kept in holes. The hydraulic diameter of hole is varied 4 in. In FloVENT, holes are created like square for the simplicity. For comparison three different volume regions are created as shown in figure below.

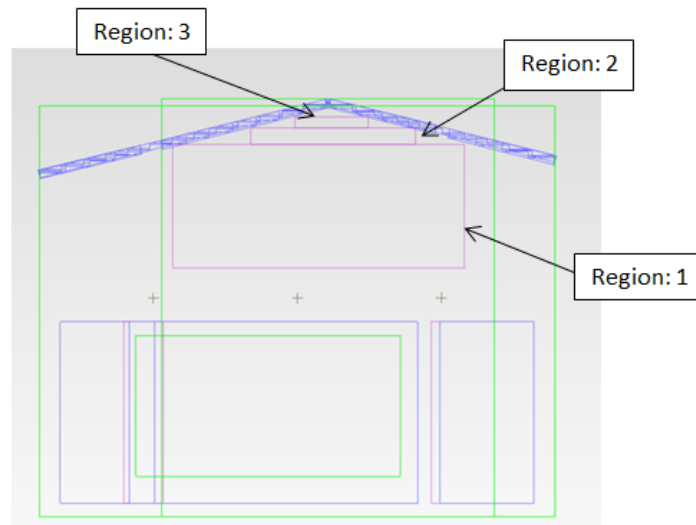


Figure 5.4 Placement of monitored volume region

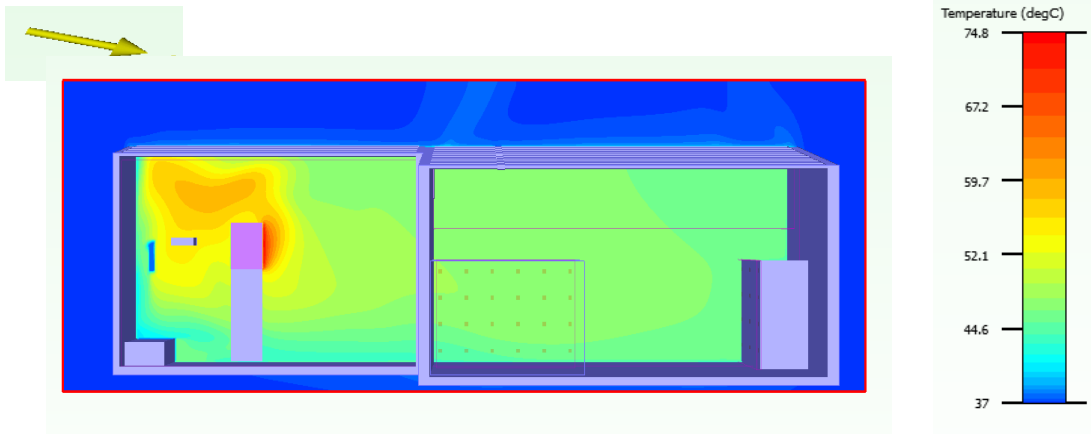


Figure 5.5 Temperature plot for summer improved model

Mean temperature is found to be 47.15° C. Maximum temperature reduced to 74.8° C.

Table 5.5 Monitor point's temperature for summer improved model

Monitor Point: 1	46.50°C
Monitor Point: 2	46.82°C
Monitor Point: 3	46.08°C

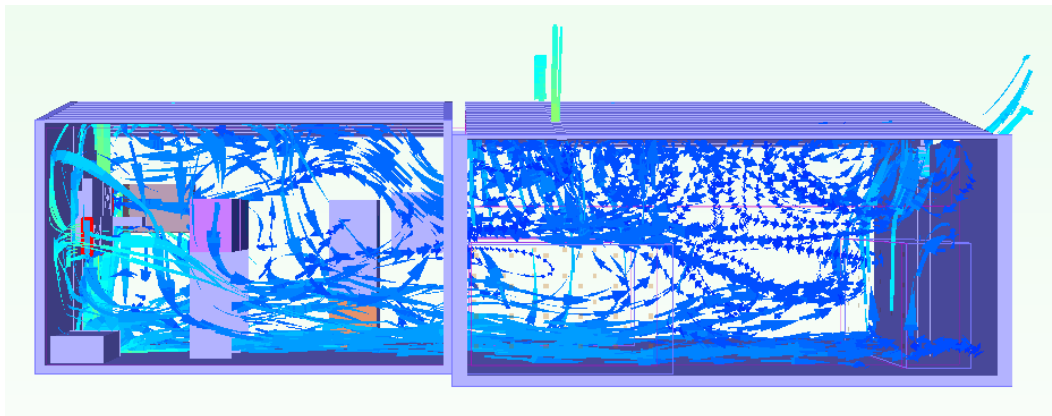


Figure 5.6 Particle trace of summer improved model

Below plot shows comparison for base and improved design in terms of concentration. Improved design helped in reducing concentration by 10% – 12%.

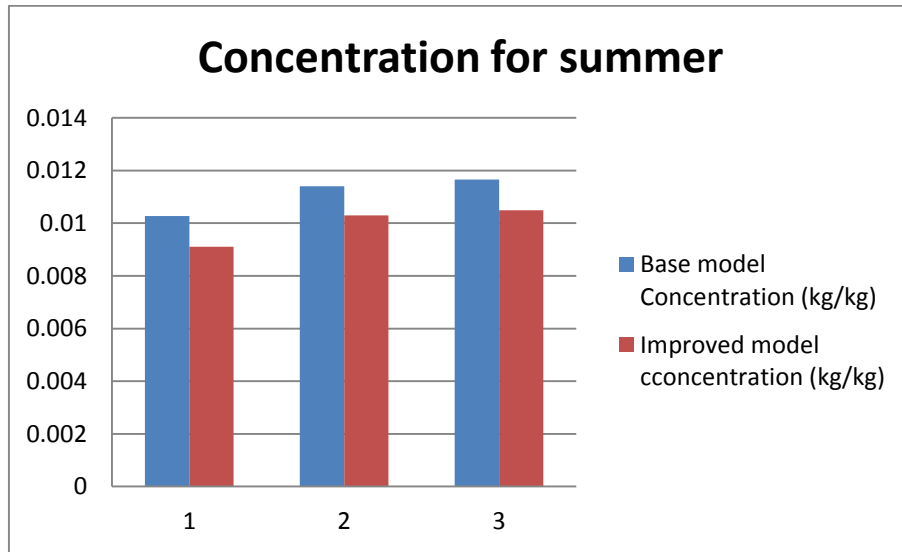


Figure 5.7 Concentration results comparison for summer

5.3 Winter model

5.3.1 Base model conditions

Ambient temperature and pressure is kept at -30° C and 20.83 in Hg respectively.

Table 5.6 Ambient condition of air for winter

Ambient temperature	-30° C
Ambient pressure	20.83 in Hg
Conductivity	0.02184 W/mK
Viscosity	1.57e-05 Ns/m ²
Density type	Ideal law
Molecular weight	28.966
Specific Heat	1007 J/Kg K

Due to -30°C inlet temperature, Inlet and outlet is closed completely. Fans are tuned off. Solver control variables are kept same as summer model. Total number of grid cells is 18 million with maximum aspect ratio of 10. As system is totally closed, it can be seen that battery temperature is increasing gradually because of accumulation of hot air and hydrogen inside the model.

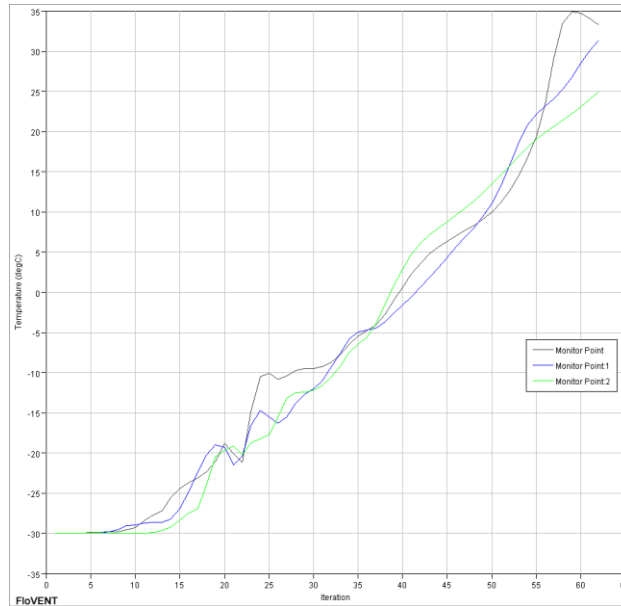


Figure 5.8 Battery temperature of winter base model

5.4 Winter improved model

Having very less temperature at inlet for winter model, it is not advisable to make it enter into model. Supplemental heating is necessary in winter season. In winter, close the inlet; IT equipment will be turned on first and then heater to get necessary warm temperature inside shelter before introducing cold air into shelter. After some time, when temperature of entire shelter will reach up to 15°C , blowers will be started at very low CFM. Blowers and heaters will be started 9if it is necessary. All this analysis needs to be done through transient analysis. For steady state analysis, it is assumed that -30°C air needs to be preheated to 15°C (heater value) before entering into shelter. So, Heater is of fixed value 15°C . Heater is placed in duct just before filet as shown in figure 5.10 below.

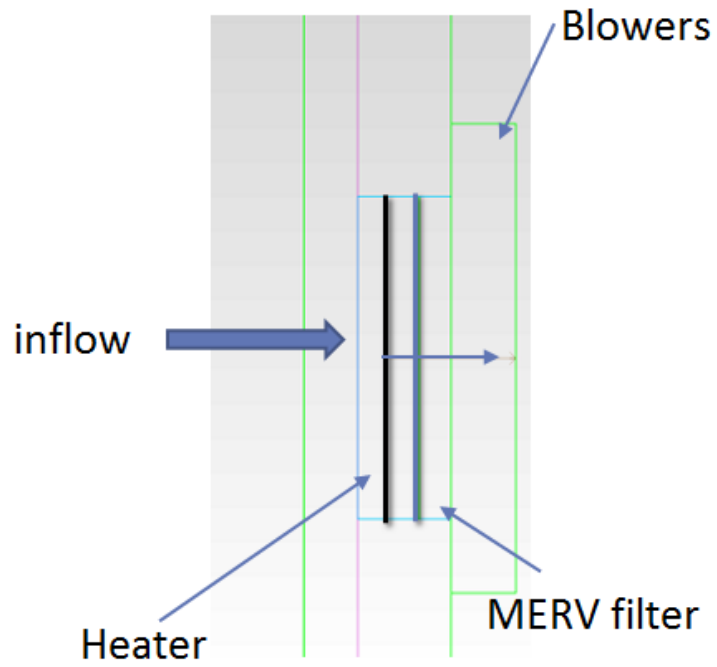


Figure 5.9 Placement of heater

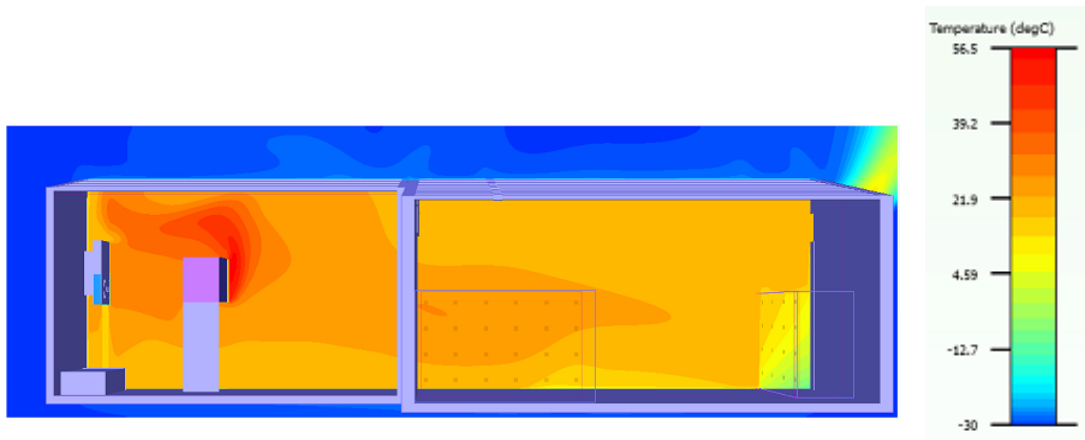


Figure 5.10 Temperature plot for winter improved model

Mean temperature is found to be 20.0° C. Maximum temperature is 56.3° C.

Table 5.7 Monitor point's temperature for winter improved model

Monitor Point: 1	20.9° C
Monitor Point: 2	21.9° C
Monitor Point: 3	21.3° C

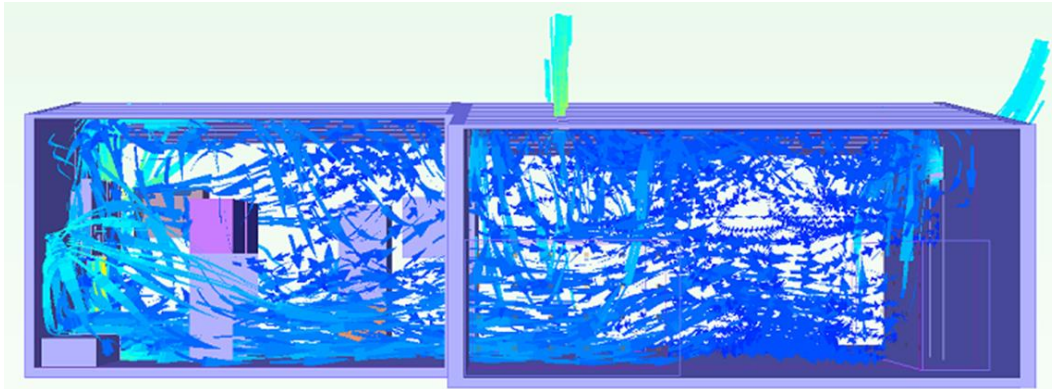


Figure 5.11 Particle trace for winter improved model

Below plot shows concentration in winter for improved in terms of regions. It is shown that maximum concentration found is 1.04% by mass.

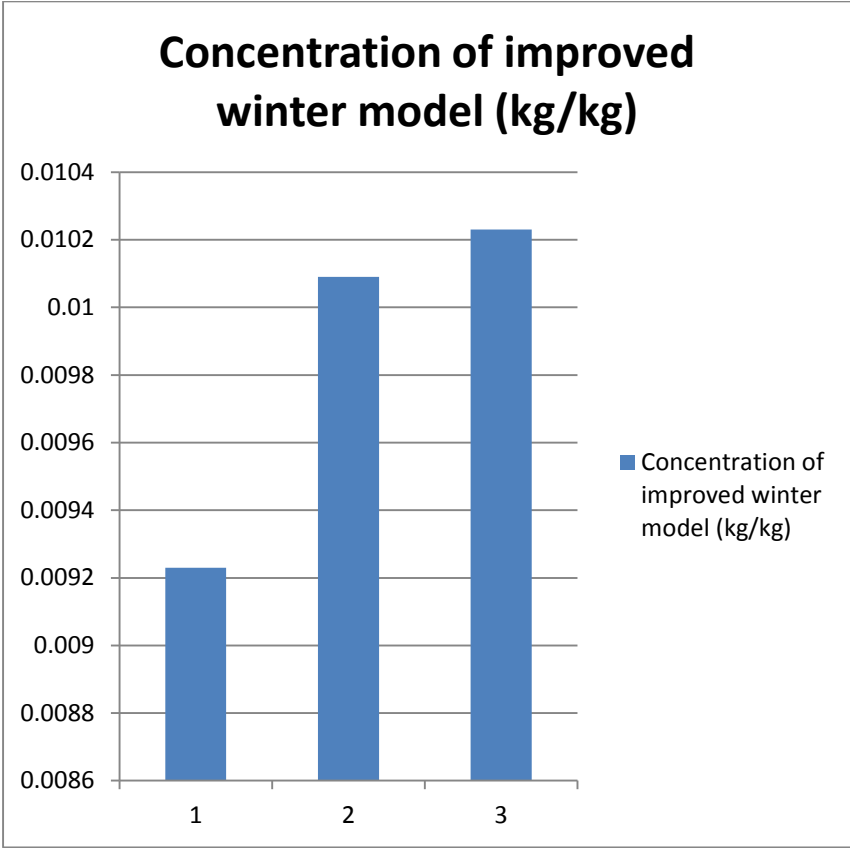


Figure 5.12 Concentration for winter improved model

Chapter 6

Conclusion and future work

6.1 Conclusion and Discussion

Steady state analysis has been performed on initial design for battery compartment. It has been observed from results that hot air and hydrogen accumulation near roof is reduced to certain level. Improved design has cooling product inlet blowers, two holes on roof, and exhaust gravity dampers at top. Exhaust gravity dampers is tested to understand the behavior of it.

- Battery temperature is found to be 46°- 47°C for summer and 20°-21°C for winter which is within ideal operating range for batteries even though after considering solar load. (0° C to 50° C).
- Supplement heating of fixed temperature 15°C is necessary in winter as ambient air temperature is very low - 30° C.
- Numerical analysis is validated by experiment on exhaust with 8% error.
- Hydrogen evacuation is reduced 10%-12% by volume in improved design for summer.
- Mean temperature of shelter is found to be 47° C for summer and 15° C for winter which is within range for electronic equipment working condition.(-20° C to 50° C)
- Maximum temperature of shelter is reduced by 10°C for summer case.
- Maximum Hydrogen evacuation is found to be 1.04 by mass for summer and winter.

6.2 Future work

Transient analysis needs to done at least for winter to see behavior of hot air and Hydrogen with solar cycle, cooling cycle for shelter, thermal power cycle, ambient condition cycle, battery hydrogen generation cycle. Also, heater location and heater temperature needs to be optimized.

Time after which ventilation is needed has to be calculated. One can try ventilation by exhaust fan instead of gravity dampers.

References

- [1] D. Agonafer, L. Gan-Li and D. B. Spalding, "The LEVEL Turbulence Model for Conjugate Heat Transfer at Low Reynolds Numbers", EEP-Vol. 18, Application of CAE/CAD Electronic Systems. ASME 1996
- [2] K.K. Dhinsa, C.J. Bailey and K.A. Pericleous, "Turbulence Modelling and it's Impact on CFD Predictions for Cooling of Electronic Components", Thermal and Thermomechanical Phenomena in Electronic Systems IThERM, 2004, pp. 487-494.
- [3] <http://www.mouser.com/ds/2/120/R1G280-275542.pdf>
- [4] http://www.efqinc.com/pdf/AIRGUARD_Legacy.pdf
- [5] www.comairtron.com major DC
- [6] ASHRAE books titled particulate and gaseous contaminants in datacom environment
- [7] <http://www.airnav.com/airport/kgjt>
- [8] Instruction manual for AMCA 210-99 air flow bench chamber
- [9] FloVENT user guide
- [10] [Support.mentorgraphics.com](http://support.mentorgraphics.com)
- [11] Telecordia GR-287
- [12] Cooling of remote sites telecommunication shelters by Abdelkader darwiche and Samivullah Shaik
- [13] ASHARE fundamental handbook 2005
- [14] Heat density trends in Data Processing, Computer Systems, a Telecommunications, (2005- 2010) White paper, Uptime Institute Inc.
- [15] <http://webparts.mentor.com/flotherm/support/webparts.jsp>
- [16] <http://webparts.mentor.com/flotherm/support/supp/advtopics/outdoorcabinet/>
- [17] Multi objective thermal and energy based design optimization of telecommunication cabinets/shelters by Muralidharan, Bharathkrishnan.

Biographical information

Palak Patel received her Bachelor's Degree in Aerospace Engineering from Gujarat Technological University in June 2013. She received her Master of Science degree in Mechanical engineering from University of Texas at Arlington in May 2015.

During her Graduate program she conducted her research in the field of thermal management under Dr.Derege Agonafer. She has indulged herself in various industry collaborated projects and gained extensive experience working in laboratory environment.

She has worked on cooling and ventilation requirement of telecommunication shelter. She conducted experiment on gravity ventilation chosen for this study.